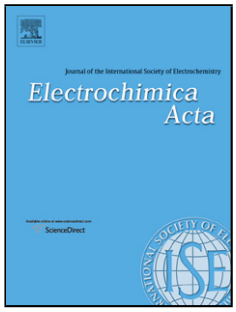

Title: Au-IDA MICROELECTRODES MODIFIED WITH Au-DOPED GRAPHENE OXIDE FOR THE SIMULTANEOUS DETERMINATION OF URIC ACID AND ASCORBIC ACID IN URINE SAMPLES

Author: <ce:author id="aut0005" author-id="S0013468616326913-8620aeaf9837aedbe0375b0af23571e3"> A. Abellán-Llobregat<ce:author id="aut0010" author-id="S0013468616326913-9aefcdebeabbf051035fe9a509131611"> L. Vidal<ce:author id="aut0015" author-id="S0013468616326913-ee92d27a535ab551a856bf2cd3f09c3a"> R. Rodríguez-Amaro<ce:author id="aut0020" author-id="S0013468616326913-29710183585cc50e4866a47d61a61a08"> Á. Berenguer-Murcia<ce:author id="aut0025" author-id="S0013468616326913-fc369351a09142fa7fa09aebd9e2fbb9"> A. Canals<ce:author id="aut0030" author-id="S0013468616326913-3a17beb31fe0b703120fedc652b99929"> E. Morallón

PII: S0013-4686(16)32691-3
DOI: http://dx.doi.org/doi:10.1016/j.electacta.2016.12.132
Reference: EA 28604

To appear in: *Electrochimica Acta*

Received date: 21-9-2016
Revised date: 16-11-2016
Accepted date: 22-12-2016

Please cite this article as: {http://dx.doi.org/

Au-IDA MICROELECTRODES MODIFIED WITH Au-DOPED GRAPHENE OXIDE FOR THE SIMULTANEOUS DETERMINATION OF URIC ACID AND ASCORBIC ACID IN URINE SAMPLES

A. Abellán-Llobregat[1], L. Vidal[2], R. Rodríguez-Amaro[3], Á. Berenguer-Murcia[1], A. Canals[2], E. Morallón[1,*]

[1]Instituto Universitario de Materiales. Universidad de Alicante. Apartado 99. 03080 Alicante. Spain.
[2]Departamento de Química Analítica, Nutrición y Bromatología e Instituto Universitario de Materiales. Universidad de Alicante. Apartado 99. 03080 Alicante. Spain.
[3]Departamento de Química Física y Termodinámica Aplicada. Universidad de Córdoba. Campus de Rabanales, C3, E14014. Córdoba. Spain.

*Corresponding author: morallon@ua.es

Telf: +34-965909590

ABSTRACT

An electrochemical sensor based on graphene oxide decorated with gold nanoparticles has been prepared for the simultaneous quantification of uric acid (UA) and ascorbic acid (AA) in urine samples. The gold interdigitated microelectrodes array (Au-IDA) has been modified using graphene oxide doped with gold nanoparticles (AuNPs-GO/Au-IDA), which was characterized by TEM, FE-SEM, XPS and cyclic voltammetry Excellent results were obtained for the separate quantification of UA and AA by chronoamperometry. The electrochemical sensor exhibits limits of detection (LODs) of 1.4 μM and 0.62 μM for AA and UA, respectively, limits of quantification (LOQs) of 4.6 μM (AA) and 2.0 μM (UA), and the working ranges obtained were between 4.6 μM and 193 μM for AA and between 2 μM and 1.05 mM for UA. The repeatability was studied at 20 μM providing coefficients of variation of 16 % for AA and 13 % for UA. Moreover UA does not interfere in the measurement of AA and viceversa (provided that the concentration of UA is equal to or higher than 450 μM in the latter case). For lower concentrations of UA, an easy and fast strategy to quantify both analytes is presented. The good electrocatalytic activity achieved with this material makes it useful for the quantification of AA and UA in biological fluids. Other analytes like glucose, dopamine and epinephrine have been investigated. The results allow us to conclude that they do not interfere in the quantification of AA and UA in PBS (0.25 M, pH 7.0). Human urine samples have been analyzed using the method proposed, contaning AA and UA

concentration levels of (0.588 ± 0.002) mM and (1.43 ± 0.02) mM, respectively, which are in the concentration range of these analytes in urine samples for healthy people.

Keywords: electrochemical sensors; graphene oxide; gold nanoparticles; uric acid; ascorbic acid

1. Introduction

Uric acid (UA; 7,9-dihydro-1H-purine-2,6,8(3H)-trione) is a weak acid present in extracellular fluids as sodium urate. Since anomalous UA levels in biological fluids have been linked to several diseases, researchers have developed several methods to detect it. Some illnesses like gout, hypertension, and cardiovascular disease, have been related to UA serum concentrations over 420 μM [1]. Other conditions like neurodegenerative diseases may be caused by UA concentrations lower than 120 μM [2]. Thus, UA normal levels in serum are established between 120 and 420 μM, with slight variations depending on the gender. Since recent studies have provided evidences that altered levels of UA in serum might have a role in the development of disease states [3], the manipulation of serum UA levels has been employed in the treatment of a variety of diseases [4]. Consequently, the development of a method to reliably quantify UA concentration in biological fluids has acquired increasing interest during the last decades.

As UA can be oxidised at common electrodes in aqueous solution, electrochemical sensors have been widely used for UA detection due to their advantages such as short analysis times, simple experimental procedures, and economical instrumentation. However, the main disadvantage for the quantification of UA in biological fluids by electrochemical sensors is the presence of species whose oxidation takes place at potentials near the UA oxidation potential on most of the common electrodes. This occurs with the oxidation of ascorbic acid (AA), resulting in a poor selectivity towards UA [5].

Moreover, the determination of AA in biological fluids is also very interesting, since it is well-known that AA is related to some diseases, and that it cannot be synthetized by

humans and it should be incorporated via diet [6]. A normal range of AA concentrations in plasma has been set between 50 and 80 μM [7,8]. An insufficient amount of AA causes symptoms of scurvy [9], but high concentrations results in gastric irritations [10]. Furthermore, AA has an important role in healthy cell development, normal tissue growth, and the healing of injuries, among other biochemical functions [11]. As a result, a huge effort has been done in order to detect and quantify both analytes separately and simultaneously in biological fluids, such as plasma or urine.

Electrochemical sensors based on carbon materials are commonly used for their low cost, good chemical stability, good electron transfer kinetics, and biocompatibility. Specifically, graphene and its derivatives have been widely used in electrochemical sensors due to their physical and electrochemical properties [12]. At present, the use of graphene oxide (GO), the oxygenated derivative of graphene, is the most promising material for the preparation of colloidal suspensions due to oxygen-containing functional groups on its surface, which provide hydrophilicity [13], facilitating its dispersion in aqueous media, and conferring high tolerance towards chemical modification [14]. As a result of the easy processing and handling of GO and its electrochemical flexibility, most of the recent efforts in the electrochemical carbon-based sensors have been based on this material. The advantages of GO allow the preparation of more concentrated dispersions, resulting in a shorter time for electrode modification. Moreover, the oxygen functional groups are amenable for bioconjugation toward the construction of biosensors, immunosensors and other devices [12]. The oxygen functional groups on GO can be reduced and regenerated electrochemically [15] with better electrical properties, high density of defects, and edge-like planes. Such combined properties enhance fast electron transfer, enabling its application in electrochemical sensing and biosensing. In order to increase its sensitivity and selectivity, GO usually is functionalised with other materials, such as nanoparticles or polymers [16–21]. At present, several of the recent studies have combined gold nanoparticles with graphene-based materials for electrochemical sensors and biosensors, trying to take advantage of the catalytic character and biocompatibility of gold. The presence of surface oxygen groups in GO increases the interaction between the metal catalyst and support [13].

The detection and quantification of UA and AA have been performed by differential pulse voltammetry (DPV) with an electrochemical sensor based on graphene oxide modified with gold nanoparticles, achieving limit of detection (LOD) of 20 μM and 200

μM, respectively [22]. However, the LOD obtained for AA should be improved due to the fact that levels of AA in plasma for healthy people are usually lower [7,8] and the detection of concentrations lower than 20 μM is also interesting [8,23]. The simultaneous determination of AA and UA within other compounds has been evaluated using a sensor based on overoxidized polyimidazole and graphene oxide copolymer by cyclic voltammetry [24]. The proposed sensor exhibited a linear response range for AA between 75 μM and 2275 μM, and for UA between 3.6 μM and 249.6 μM. Several works have been reported for the electroanalytical determination of UA and AA in the presence of other compounds and most of them used a glassy carbon electrode as support of the modified-GO [17,18,20]. Benvidi et al. fabricated a reduced graphene oxide (RGO), gold nanoparticles and 2-(3,4-dihydroxyphenyl)benzothiazole-modified glassy carbon electrode for the simultaneous determination of levodopa, uric acid and folic acid [17]. Only a few publications may be found related with modified interdigitated arrays [21,25] or screen-printed electrodes [19], with a small size which makes the development of portable Lab-on-a-Chip devices feasible.

The aim of the present work is the preparation by a one-step method of an electroactive material based on graphene oxide with gold nanoparticles with low loadings supported on gold interdigitated microelectrodes. Gold nanoparticles were synthesized following a method which allow not only fine nanoparticle size and distribution control but also avoid the use of additional reducing agents, improving the cost-efficiency of the synthetic process [26]. The modified electrodes have been assessed in the simultaneous detection and quantification of AA and UA in biological fluids, also improving the limits of detection hitherto achieved by using graphene oxide as support of metallic nanoparticles. To the best of our knowledge, this is the first time that an interdigitated electrode array is modified with Au-decorated graphene oxide sample, allowing the development of portable sensors for the simultaneous UA and AA determination.

2. Experimental

2.1. Reagents and equipment

Uric acid (≥99%, crystalline) and L-Ascorbic acid (reagent grade, crystalline), dopamine hydrochloride, glucose and epinephrine standard chemicals, glutaraldehyde (50%) and poly(styrenesulfonate) (PSS) were provided by Sigma-Aldrich. Potassium dihydrogen phosphate (KH_2PO_4) and Potassium phosphate dibasic (K_2HPO_4) obtained

from Emsure® and Sigma-Aldrich respectively, were used to prepare buffer solution (PBS, 0.25 M, pH 7.0). Sulphuric acid (98%) was provided by AnalaRNormapur®. Ultrapure water was obtained by a treatment in Purelab Ultra Elga with a resistivity of 18 MΩ·cm. Sodium hydroxide proanalysis (NaOH) was purchased from Merck.
The reagents employed in the gold nanoparticles synthesis, (poly-n-vinylpyrrolidone (PVP), anhydrous ethylene glycol, sodium tetrachloroaurate dehydrate ($NaAuCl_4 \cdot 2H_2O$), methanol and sodium hydroxide (NaOH; 99.99% purity) were purchased from Sigma-Aldrich. Isopore Membrane Filters (0.2 μm GTTP) from Millipore were employed for cleaning and drying of the material synthesized and absolute ethanol was purchased from PROLABO.
Transmission electron microscopic measurements (TEM) were carried out using a JEOL TEM, JEM-2010 model equipped with an Oxford X-ray detector (EDS), INCA Energy TEM 100 model, and GATAN acquisition camera. Scanning electron micrographs (SEM) were taken using an ORIUS SC600 model Field Emission Scanning Electron Microscope (FE-SEM) using a ZEISS microscope, Merlin VP Compact model, with an EDX Bruker, Quantax 400 model.
X-ray photoelectron spectroscopy (XPS) was performed using a VG-Microtech Multilab 3000 spectrometer using non-monochromatised MgKα (1253.6 eV) radiation from a twin anode source operated at 300 W (20 mA, 15 kV). Photoelectrons were collected into a hemispherical analyser working in the constant energy mode at pass energy of 50 eV. The binding energy (BE) of the Cls peak at 286.4 eV was taken as internal standard.

2.2. Preparation of graphene oxide decorated with gold nanoparticles

2.2.1. Synthesis and purification of graphene oxide decorated with gold nanoparticles

Graphene oxide was prepared following the Hummers method improved by Marcano et al. [27].
Gold nanoparticles were synthesized following a method based in the methodology described by Dominguez et al.[26] with several modifications which allow not only fine nanoparticle size and distribution control (as most chemical methods for the synthesis of metallic colloids, which represents a significant advantage over other methods) but also avoid the use of additional reducing agents, improving the cost-efficiency of the

synthetic process. In order to control the nanoparticle size and to obtain a good size distribution, the synthesis was performed in an inert atmosphere in a Schlenk system unless stated otherwise.

In order to decorate the graphene oxide support with a 10% (w/w) of gold nanoparticles, the following method was applied. For solution 1, in a two-necked, round-bottom flask, 0.075 g of graphene oxide and 0.120 g of poly-n-vynilpyrrolidone were added to 12 mL of anhydrous ethylene glycol. The mixture was maintained at 80ºC under stirring conditions for 1 h. For solution 2, in a two-necked, round-bottom flask, 0.022 g of gold precursor ($NaAuCl_4 \cdot 2H_2O$) were dissolved in 5 mL of methanol under stirring at room temperature during 1 h. The resulting solution was of yellow color.

After that, solution 1 was cooled at 0ºC with an ice bath and solution 2 was added to solution 1, keeping the stirring to ensure a good homogenization. The pH of the resulting solution was adjusted to 9-10 by adding 0.5 mL of a NaOH 1 M solution and the resulting solution was heated at 100 ºC under vigorous stirring for 2 h. After 2 hours the flask was removed from the bath and cooled to room temperature.

The GO decorated with AuNPs was purified with a vacuum filtration system. The sample on the filter was cleaned with an excess of ethanol and the solid obtained was dried in a vacuum oven at 40ºC for 24 h.

2.2.2. Graphene oxide decorated with gold nanoparticles dispersion

Dispersions of 1 $mg \cdot mL^{-1}$ of graphene oxide (GO) and graphene oxide modified with gold nanoparticles (AuNPs-GO) were prepared in water. Both dispersions contained 1% PSS in order to achieve the dispersion of the carbon material. To obtain a proper dispersion, an ultrasound probe was applied for 10 min (QSonica, MODEL Q125, 100W). In order to avoid localized heating during sonication, the vessels containing the sample suspensions were immersed in an ice bath.

2.3. Preparation of Au-IDA modified electrodes

First, cyclic voltammetry was performed in order to clean the gold (thin film of 150 nm) interdigitated microelectrodes array (Au-IDA1, Micrux). The size of the working electrode is 10 µm. Then, ten cycles between -1.5 V and 1.5 V versus the gold pseudo-reference at 0.1 V s^{-1} in 0.05 M H_2SO_4 were applied.

Then the Au-IDA microelectrode was modified by casting the aqueous AuNPs-GO dispersion obtaining the AuNPs-GO/Au-IDA modified electrode. An Au-IDA modified electrode with GO was also prepared for electrochemical characterization. In both kinds of electrodes, the weight of the graphene oxide-based material deposited was 5 μg. The method for the deposition was the dropwise addition of 0.5 μL of each dispersion and drying under an infrared lamp. Finally, 0.75 μL of glutaraldehyde were added to ensure that the solid material remains on the surface of the Au-IDA electrode. The scheme shown in Figure 1 illustrates the preparation procedure for the sensor electrode.

2.4. Electrochemical methods

All electrochemical measurements were carried out on a BIOLOGIC SP-300 potentiostat. A three-electrode configuration was used, in which the electrode modified with graphene oxide-based material was the working electrode (WE), a reversible hydrogen electrode (RHE) was the reference electrode (RE) and a platinum wire was the counter electrode (CE). The electrochemical cell was completely deoxygenated during measurements by bubbling nitrogen. All potentials presented are referred to the RHE electrode.

To identify the analytes, cyclic voltammetry was carried out in order to know at which potential the oxidation of UA and AA occurs. For that, a concentrated stock UA solution (100 mM) was prepared in PBS (0.25 M, pH 7.0) at a pH higher than 8.4 and then diluted ten times. A concentrated stock AA solution (135 mM) was also prepared. Three different aliquots from the stock solutions were added to the electrochemical cell to reach the desired concentration (C_{AA} = 75, 175 and 275 μM; C_{UA} = 200, 400 and 600 μM). Afterwards, cyclic voltammetry was applied between 0.3 V and 1.3 V.

Quantification of UA and AA was carried out by chronoamperometry. A total of fourteen aliquots of UA were added reaching concentrations between 0.62 μM and 1 mM. For AA, twenty-two AA additions were performed, in the concentration range between 1.4 μM and 3 mM. Stirring was kept during the experiments to ensure a good homogenization. All measurements were carried out in PBS (0.25 M, pH 7.0) and by triplicate in order to determine analytical parameters.

It is important to highlight that since the pH of the physiological fluids employed is higher than the pKa_1 of these analytes, the quantification of ascorbate monoanion (HA^-)

[8] and urate (HU^-) [28] has been determined. However, these analytes will be referred to as AA and UA throughout the manuscript, respectively.
For real samples determination, filtered urine was diluted 20 times in PBS (0.25 M, pH 7.0) and no other treatment was carried out.

3. Results and Discussion

3.1. AuNPs-GO/Au-IDA electrodes characterization

3.1.1. Electrochemical characterization

The electrochemical behavior of GO/Au-IDA and AuNPs-GO/Au-IDA electrodes was studied by cyclic voltammetry in PBS (0.25 M, pH 7.0). Figure 2 depicts the voltammograms registered between 0.0 V and 1.8 V with a scan rate of 0.1 V s^{-1}. Twelve cycles between 0.0 V and 1.8 V were performed and from cycle 8 the steady voltammograms were obtained.
For GO/Au-IDA electrode (Figure 2, dashed line), the formation of the electrical double layer is manifested by the rectangular shape of the voltammogram between 0.5 V and 1.8 V. For AuNPs-GO/Au-IDA electrode (solid line in Figure 2), the oxidation process of the gold surface at 1.5 V is observed during the positive scan and the reduction peak at 1.1 V related to the desorption of oxygen from the gold surface can be clearly seen. In addition, a high cathodic current can be seen due to the electrocatalytic effect of the AuNPs in the hydrogen reduction reaction on the gold surface.

3.1.2. Structural characterization

Figure 3 shows two representative TEM images for the GO and the AuNPs-GO dispersions. As it can be seen in Figure 3A, single layer structured GO flakes with a smooth surface were provided. The TEM micrograph of AuNPs-GO dispersion (Figure 3B) shows a uniform distribution of the AuNPs on GO surface, with an average particle size between 4-9 nm, as shown in the histogram (Figure 3C). The presence of wrinkles in Figure 3A is an evidence of the conformational flexibility of GO, which is the reason why GO is locally folded in double or multiple layers [29].

The surface morphology of the modified electrode (AuNPs-GO/Au-IDA) was characterized by FE-SEM. Figure 4 presents a material with several layers of graphene. The spots observed in Figure 4 correspond to the AuNPs. It can be observed that the

nanoparticles are homogeneously distributed on the electrode, and the entire Au-IDA electrode surface is covered. Figure 4 also shows the same sheet wrinkling, which indicates the presence of several layers of GO.

XPS was used in order to determine the state of the main constituents of the dispersion (namely, Au, C, and O). The elemental contents of carbon, oxygen and gold were also quantified for both dispersions. Figure 5 shows the XPS spectra of gold for the AuNPs-GO dispersion, in which a single peak appears for the Au $4f_{7/2}$ and Au $4f_{5/2}$ signals which may be assigned to zerovalent gold. The results for the pristine GO dispersion had a carbon and oxygen contents of, 80 wt% and 20 wt%, respectively. For the AuNPs-GO dispersion the XPS results showed a 1.9 wt% of gold, 81.3 wt% of carbon and 16.8 wt% of oxygen in the sample. Comparing the amount of oxygen in both dispersions a decrease in the amount of oxygen after gold nanoparticles were synthetized on GO (20 wt% for GO dispersion vs 16.8 wt% for AuNPs-GO dispersion) can be seen, which may be ascribed to the presence of the metallic particles. This observation is corroborated by the fact that the C1s XPS spectra for both samples (results not shown) were very similar, with negligible variations in the relative intensities of the peaks which may be ascribed to graphitic carbon (peak at 284.9 eV), phenol or ether-related groups (286.3 eV), quinone-related groups (287.5 eV), and carboxyl or ester-related groups (288.9 eV) [30].

3.2. Electrochemical determination of AA and UA on AuNPs-GO/Au-IDA electrodes.

The electrochemical oxidation activity of AuNPs-GO/Au-IDA modified electrode towards UA and AA was investigated. Figure 6 shows the voltammograms obtained for three concentrations of AA (Figure 6A) and UA (Figure 6B). A peak around 0.7 V due to the oxidation of AA (Figure 6A) and a peak around 1.0 V related to the oxidation of UA (Figure 6B) can be observed. In order to minimize any possible interferences usually found in biological fluids, the oxidation potentials selected for AA (0.75 V) and UA (1.0 V) detection by amperometric methods were the minimum possible without causing a substantial sensitivity decrease in the detection of either AA or UA, respectively.

Figure 7 exhibits the amperometric response of AuNPs-GO/Au-IDA electrode towards the several additions of AA and UA in PBS (0.25 M, pH 7.0). Figures 7A-B show the i-t curves obtained with the modified electrode towards AA additions at a fixed potential of 0.75 V. The corresponding calibration curve obtained is shown in Figure 8A. As it can be observed in Figure 8A (inset), the analytical range studied seems to be characterized by two linear ranges, which means that the functional relationship is not linear at all. The reduction of the concentration range is one of the most widespread strategies to solve this [31]. To achieve this, a working response range between 4.6 μM and 193 μM is established, with a LOD and LOQ of 1.4 μM and 4.6 μM, respectively. The linear regression function is: i_{AA} (nA) = (830 ± 60) C_{AA} (mM) + (7 ± 5); with a correlation coefficient given by r = 0.996 (N = 10).
In Figures 7C-D, the i-t curves obtained at 1.0 V for successive aliquots of UA can be observed, and the corresponding calibration curve is plotted in Figure 8B. A working response range was found for UA oxidation between 2 μM and 1.05 mM. The LOD and LOQ obtained were 0.62 μM and 2 μM, respectively. The linear equation is next given by: i_{UA} (nA) = (728±16) C_{UA} (mM) + (13± 7); r = 0.999 (N = 12).

All analytical figures of merit calculated for the quantification of AA and UA are summarized in Table 1. The LOD was determined empirically, measuring progressively more diluted concentrations of the analyte. The LOD was the lowest concentration whose signal could be clearly distinguished from the blank. Moreover, the LOQ was calculated as 3.3 times the LOD (LOQ = 3.3LOD) [32]. The coefficient of variation values (CV) were obtained for 3 replicates at 20 μM concentration level of UA and AA.

3.3. Simultaneous detection of AA and UA

In order to study the simultaneous detection of AA and UA, cyclic voltammetry was performed in a solution containing the two analytes. Figure 9 shows the voltammograms obtained for the AA and UA interference study. Figure 9A displays the behavior of AuNPs-GO/Au-IDA electrode for a UA concentration of 600 μM and successive aliquots from a stock solution of AA until reaching concentrations between 30 and 90 μM. The voltammograms obtained do not show differences after the additions of AA in this range of concentrations.

The results obtained for the addition of UA aliquots in a solution containing 275 μM AA are presented in Figure 9B. As it is exhibited in the voltammetric curves, the current of the voltammetric peak owing to AA oxidation (E = 0.75 V) decreased after UA aliquots were added. Then, it seems that UA interferes in the voltammetric response of AA. Then, the amperometric responses for minimum and maximum levels of AA and UA were determined to have a broad knowledge about how each analyte interferes in the determination of the other.

The interference study of UA and AA has been performed by chronoamperometry at 0.75 V and 1.0 V, respectively and with concentrations higher than the normal values in serum. Figure 10 and Figure 11 display the i-t curves recorded for the interference study. Figure 10 evidences the effect of the addition of UA with a concentration between 120 μM and 1.0 mM in the current at 0.75 V when the concentration of AA is 30 μM (Figure 10A) and 90 μM (Figure 10B), respectively in the PBS solution. As it can be observed, additions of UA with a concentration within the established lineal range (120-1000 μM), do not change the intensity of the AA oxidation current measured at 0.75 V. Thus, the present method should be able to quantify AA with UA being present in the serum samples.

On the other hand, Figure 11 shows the effect of the addition of AA with a concentration between 30 μM and 90 μM in the UA oxidation current at 1.0 V when the UA concentration is 120 μM (Figure 11A) or 450 μM (Figure 11B) in the solution. It can be observed for the lowest UA concentration established in serum (120 μM, Figure 11A) that additions of AA lead to an increase on the current measured at 1.0 V potential. That means that AA interferes in the quantification of low concentrations of UA.

However, when the UA concentration is the highest allowed for healthy people (around 450 μM), Figure 11B depicts how the AA additions lead to a small increase in the measured current (21, 11 and 33 nA for the 1st, 2nd and 3rd aliquot, respectively). Taking into account that confidence limits for this concentration values are about ± 30 nA, this increase can be considered included in the experimental error of the measurements. As a result, this method is able to quantify UA in unhealthy people (UA concentration at least 450 μM) in presence of AA up to a concentration of 60 μM.

In order to apply the present method to healthy people, whose UA levels are lower than 450 μM, the following strategy may be applied: 1) calibration curve of AA at 0.75 V, 2) calibration curve of UA in the presence of the amount of AA in the real sample at 1.0 V potential. Preparation of calibration curve 2 requires knowing the concentration of AA in the sample beforehand. In order to avoid the preparation of a calibration curve (i-t curve at 1.0 V) after knowing the amount of AA present in the real sample, it becomes advisable to prepare several i-t curves with different AA concentrations between 10 μM and150 μM. Thus, the method can be applied in people with AA levels lower or higher than the fixed range levels. The sample, which contains a mixture of AA and UA will be subjected to chronoamperometry. First of all, the i-t curves at 0.75 V and 1.0 V potential of the sample will be recorded. The i-t curve at 0.75 V will provide a current intensity value ($i_{AA,1}$), which is directly related to the concentration of AA (C_{AA}) by the linear function of calibrate curve 1. From the i-t curve at 1.0 V, a second current value ($i_T = i_{AA,2} + i_{UA}$) will be obtained, from which the amount of UA in the sample can be quantified by using the linear function of calibrate curve 2, which has been made with the amount of AA that was present in the real sample.

3.4. Study of other interferences

Other possible interferences, like glucose, dopamine (DP) and epinephrine (EP) were investigated by chronoamperometry at 0.75 V and 1.0 V in PBS (0.25 M, pH 7.0), to know if the presence of these analytes in physiological fluids are able to modify the signal belonging to the oxidation of AA and UA.

In order to study the interference of these compounds, concentrations of glucose (5 mM) [33], dopamine (1 μM) [34], [35] and epinhefrine (0.5 μM) were used, being these concentrations higher than the usually found in serum [36], [37]. Interferences at 0.75 V and 1.0 V were investigated in a 50 μM AA solution and 420 μM UA solution, respectively, being these concentrations usually found in serum, and the results obtained are displayed in Figure 12.

As it can be observed in Figure 12 the addition of glucose, dopamine and epinephrine does not change the current intensity corresponding to the oxidation of AA at 0.75 V (Figure 12A) and UA at 1.0 V (Figure 12B). As a result of that, it can be concluded that

the method developed is able to quantify AA and UA, even in the presence of the analytes studied above.

Finally, Table 2 shows a comparison of some analytical parameters obtained in this work, with others results previously reported. It can be observed that the proposed sensor is competitive, representing therefore a good and interesting alternative. Moreover, the LODs and LOQs achieved with the proposed sensor are greatly improved with respect to those shown in a recent publication about this topic [22], whose similarity lies in the same electrode material.

3.5. Human urine samples

A human urine sample from a healthy person was analyzed by the standard addition method due to matrix effects, which caused the displacement of the oxidation peaks related to AA and UA to more positive potentials (results not shown). Despite the fact that the possible interferences have been studied in PBS with proper results, urine is a complex matrix with several components like proteins that can block the active sites on the electrode. Filtered urine was diluted 20 times in PBS (0.25 M, pH 7.0) and no other treatment was carried out.

For this reason the calibration curves for AA and UA were obtained by chronoamperometry at 0.95 V and 1.2 V, respectively, for the same concentrations of AA and UA studied in Figure 7. The concentration of AA determined was 0.588 ± 0.002 mM or 155.3 ± 0.7 mg/24 h (based on a 1.5 L total urine volume in 24 hours [45]). The average AA value excreted by urine in 24 hours has been determined in 34 mg. However, that value can be changeable, and for example, a high concentration of 450 mg/24 h has been found after the ingestion of 700 mg of AA [46]. For that reason, the AA concentration found in the present work is not surprising.

On the other hand, the urine sample had a concentration of 1.43 ± 0.02 mM of UA or 361 ± 5 mg/24 h, values which are within the normal levels of UA (200-2000 mg/24 h [47] or 1.4 - 3.3 mM [48]).

Inter-sensor reproducibility was studied using five electrodes prepared using the method described in section 2.3. The obtained results yielded coefficients of variation (CV)

values about 27% for AA and about 9% for UA determination which prove the reliability of the developed method (Figure 13).

2. Conclusions

An electrochemical method based on the modification of an array of gold interdigitated microelectrodes by graphene oxide decorated with gold nanoparticles (AuNPs-GO/Au-IDA) has been developed for quantification of AA and UA in urine samples. In order to simulate physiological human fluids all investigations have been carried out in PBS (0.25 M, pH 7.0). The AuNPs-GO/Au-IDA modified electrode exhibits a working range of 4.6-193 μM for AA and 2-1.05 mM for UA achieving LODs of 1.4 μM and 0.62 μM, respectively. These good values make the application of the method in serum samples, or other biological fluids possible, even when the AA and UA concentrations are lower than the normal values in serum.

The simultaneous quantification of AA and UA has been investigated. No interference of UA in the AA measurements has been carried out successfully. On the other hand, AA does not interfere in the UA quantification for UA concentrations higher than 450 μM. For lower concentrations of UA, an easy and fast strategy to quantify both analytes was presented. The proposed sensor showed excellent antiinterference properties against glucose, dopamine and epinephrine and it has been favorably applied on the analysis of real urine samples.

3. Acknowledgements

This work is supported by the Generalitat Valenciana (Prometeo2013/038 and PROMETEOII/2014/010) and by the Ministerio de Economia y Competitividad (MAT2013-42007-P and CTQ2015-66080-R). A. Abellán also thanks the Generalitat Valenciana for her fellowship.

References

[1] R.J. Johnson, D.-H. Kang, D. Feig, S. Kivlighn, J. Kanellis, S. Watanabe, K.R. Tuttle, B. Rodriguez-Iturbe, J. Herrera-Acosta, M. Mazzali, Is there a pathogenetic role for uric acid in hypertension and cardiovascular and renal disease?, Hypertension. 41 (2003) 1183–1190.
[2] I. Hisatome, M. Tsuboi, C. Shigemasa, Renal hypouricemia, Nihon Rinsho Jpn. J. Clin. Med. 54 (1996) 3337–3342.
[3] M. Mazzali, J. Hughes, Y.-G. Kim, J.A. Jefferson, D.-H. Kang, K.L. Gordon, H.Y. Lan, S. Kivlighn, R.J. Johnson, Elevated uric acid increases blood pressure in the rat by a novel crystal-independent mechanism, Hypertension. 38 (2001) 1101–1106.
[4] M.K. Kutzing, B.L. Firestein, Altered uric acid levels and disease states, J. Pharmacol. Exp. Ther. 324 (2008) 1–7.
[5] D. Lakshmi, M.J. Whitcombe, F. Davis, P.S. Sharma, B.B. Prasad, Electrochemical detection of uric acid in mixed and clinical samples: a review, Electroanalysis. 23 (2011) 305–320.
[6] V. Valpuesta, M.A. Botella, Biosynthesis of L-ascorbic acid in plants: new pathways for an old antioxidant, Trends Plant Sci. 9 (2004) 573–577.
[7] A.A. Fowler, A.A. Syed, S. Knowlson, R. Sculthorpe, D. Farthing, C. DeWilde, C.A. Farthing, T.L. Larus, E. Martin, D.F. Brophy, S. Gupta, Medical Respiratory Intensive Care Unit Nursing, B.J. Fisher, R. Natarajan, Phase I safety trial of intravenous ascorbic acid in patients with severe sepsis, J. Transl. Med. 12 (2014) 32.
[8] J. Du, J.J. Cullen, G.R. Buettner, Ascorbic acid: Chemistry, biology and the treatment of cancer, Biochim. Biophys. Acta BBA - Rev. Cancer. 1826 (2012) 443–457.
[9] S.J. Padayatty, A. Katz, Y. Wang, P. Eck, O. Kwon, J.-H. Lee, S. Chen, C. Corpe, A. Dutta, S.K. Dutta, M. Levine, Vitamin C as an antioxidant: evaluation of its role in disease prevention, J. Am. Coll. Nutr. 22 (2003) 18–35.
[10] P. b. Nunn, Oxalic acid in biology and medicine, FEBS Lett. 101 (1979) 421–421.
[11] S. Chambial, S. Dwivedi, K.K. Shukla, P.J. John, P. Sharma, Vitamin C in disease prevention and cure: an overview, Indian J. Clin. Biochem. 28 (2013) 314–328.
[12] S.K. Vashist, J.H.T. Luong, Recent advances in electrochemical biosensing schemes using graphene and graphene-based nanocomposites, Carbon. 84 (2015) 519–550.
[13] S. Stankovich, D.A. Dikin, R.D. Piner, K.A. Kohlhaas, A. Kleinhammes, Y. Jia, Y. Wu, S.T. Nguyen, R.S. Ruoff, Synthesis of graphene-based nanosheets via chemical reduction of exfoliated graphite oxide, Carbon. 45 (2007) 1558–1565.
[14] D.R. Dreyer, S. Park, C.W. Bielawski, R.S. Ruoff, The chemistry of graphene oxide, Chem. Soc. Rev. 39 (2009) 228–240.

[15] E.L.K. Chng, M. Pumera, Solid-state electrochemistry of graphene oxides: absolute quantification of reducible groups using voltammetry, Chem. – Asian J. 6 (2011) 2899–2901.
[16] K.R. Ratinac, W. Yang, J.J. Gooding, P. Thordarson, F. Braet, Graphene and related materials in electrochemical sensing, Electroanalysis. 23 (2011) 803–826.
[17] A. Benvidi, A. Dehghani-Firouzabadi, M. Mazloum-Ardakani, B.-B.F. Mirjalili, R. Zare, Electrochemical deposition of gold nanoparticles on reduced graphene oxide modified glassy carbon electrode for simultaneous determination of levodopa, uric acid and folic acid, J. Electroanal. Chem. 736 (2015) 22–29.
[18] L. Yang, N. Huang, Q. Lu, M. Liu, H. Li, Y. Zhang, S. Yao, A quadruplet electrochemical platform for ultrasensitive and simultaneous detection of ascorbic acid, dopamine, uric acid and acetaminophen based on a ferrocene derivative functional Au NPs/carbon dots nanocomposite and graphene, Anal. Chim. Acta. 903 (2016) 69–80.
[19] S. Azzouzi, L. Rotariu, A.M. Benito, W.K. Maser, M. Ben Ali, C. Bala, A novel amperometric biosensor based on gold nanoparticles anchored on reduced graphene oxide for sensitive detection of l-lactate tumor biomarker, Biosens. Bioelectron. 69 (2015) 280–286.
[20] H. Shu, G. Chang, J. Su, L. Cao, Q. Huang, Y. Zhang, T. Xia, Y. He, Single-step electrochemical deposition of high performance Au-graphene nanocomposites for nonenzymatic glucose sensing, Sens. Actuators B Chem. 220 (2015) 331–339.
[21] H.Y. Kim, K.J. Jang, M. Veerapandian, H.C. Kim, Y.T. Seo, K.N. Lee, M.-H. Lee, Reusable urine glucose sensor based on functionalized graphene oxide conjugated Au electrode with protective layers, Biotechnol. Rep. 3 (2014) 49–53.
[22] H. Imran, P.N. Manikandan, V. Dharuman, Facile and green synthesis of graphene oxide by electrical exfoliation of pencil graphite and gold nanoparticle for non-enzymatic simultaneous sensing of ascorbic acid, dopamine and uric acid, RSC Adv. 5 (2015) 63513–63520.
[23] German Nutrition Society (DGE), New reference values for vitamin C intake, Ann. Nutr. Metab. 67 (2015) 13–20.
[24] X. Liu, L. Zhang, S. Wei, S. Chen, X. Ou, Q. Lu, Overoxidized polyimidazole/graphene oxide copolymer modified electrode for the simultaneous determination of ascorbic acid, dopamine, uric acid, guanine and adenine, Biosens. Bioelectron. 57 (2014) 232–238.
[25] R. Lanche, L.E. Delle, M. Weil, X.T. Vu, V. Pachauri, W.M. Munief, P. Wagner, S. Ingebrandt, Routine fabrication of reduced graphene oxide microarray devices via all solution processing, Phys. Status Solidi A. 210 (2013) 968–974.
[26] S. Domínguez-Domínguez, J. Arias-Pardilla, Á. Berenguer-Murcia, E. Morallón, D. Cazorla-Amorós, Electrochemical deposition of platinum nanoparticles on different carbon supports and conducting polymers, J. Appl. Electrochem. 38 (2007) 259–268.
[27] D.C. Marcano, D.V. Kosynkin, J.M. Berlin, A. Sinitskii, Z. Sun, A. Slesarev, L.B. Alemany, W. Lu, J.M. Tour, Improved synthesis of graphene oxide, ACS Nano. 4 (2010) 4806–4814.
[28] Z. Wang, E. Königsberger, Solubility equilibria in the uric acid–sodium urate–water system12, Thermochim. Acta. 310 (1998) 237–242.
[29] F. Perrozzi, S. Prezioso, L. Ottaviano, Graphene oxide: from fundamentals to applications, J. Phys. Condens. Matter. 27 (2015) 13002.
[30] A.P. Terzyk, The influence of activated carbon surface chemical composition on the adsorption of acetaminophen (paracetamol) in vitro - Part II. TG, FTIR, and XPS analysis of carbons and the temperature dependence of adsorption kinetics at the neutral pH, Colloids Surf. Physicochem. Eng. Asp. 1 (2001) 23–45.

[31] E. Desimoni, B. Brunetti, Presenting Analytical Performances of Electrochemical Sensors. Some Suggestions, Electroanalysis. 25 (2013) 1645–1651.
[32] Miller, J., Miller, J.C., Statistics and chemometrics for analytical chemistry, 6th edition, Pearson, 6th edition, 2010.
[33] J. Wang, Electrochemical glucose biosensors, Chem. Rev. 108 (2008) 814–825..
[34] C.B. Jacobs, M.J. Peairs, B.J. Venton, Review: Carbon nanotube based electrochemical sensors for biomolecules, Anal. Chim. Acta. 662 (2010) 105–127.
[35] K. Hashizume, A. Yamatodani, T. Ogihara, Free and total dopamine in human plasma: effects of posture, age and some pathophysiological conditions, Hypertens. Res. 18 (1995) S205–S207.
[36] H. Devnani, S.P. Satsangee, R. Jain, A novel graphene-chitosan-Bi2O3 nanocomposite modified sensor for sensitive and selective electrochemical determination of a monoamine neurotransmitter epinephrine, Ionics. (2015) 1–14.
[37] D.S. Goldstein, G. Eisenhofer, I.J. Kopin, Sources and significance of plasma levels of catechols and their metabolites in humans, J. Pharmacol. Exp. Ther. 305 (2003) 800–811.
[38] A. Joshi, W. Schuhmann, T. C. Nagaiah, Mesoporous nitrogen containing carbon materials for the simultaneous detection of ascorbic acid, dopamine and uric acid, Sens. Actuators B Chem. 230 (2016) 544–555.
[39] M. Choukairi, D. Bouchta, L. Bounab, M. Ben atyah, R. Elkhamlichi, F. Chaouket, I. Raissouni, I.N. Rodriguez, Electrochemical detection of uric acid and ascorbic acid: Application in serum, J. Electroanal. Chem. 758 (2015) 117–124.
[40] S. Yan, X. Li, Y. Xiong, M. Wang, L. Yang, X. Liu, X. Li, L.A.M. Alshahrani, P. Liu, C. Zhang, Simultaneous determination of ascorbic acid, dopamine and uric acid using a glassy carbon electrode modified with the nickel(II)-bis(1,10-phenanthroline) complex and single-walled carbon nanotubes, Microchim. Acta. (2016) 1–8.
[41] Y. Liu, J. Huang, H. Hou, T. You, Simultaneous determination of dopamine, ascorbic acid and uric acid with electrospun carbon nanofibers modified electrode, Electrochem. Commun. 10 (2008) 1431–1434.
[42] L. Yang, D. Liu, J. Huang, T. You, Simultaneous determination of dopamine, ascorbic acid and uric acid at electrochemically reduced graphene oxide modified electrode, Sens. Actuators B Chem. 193 (2014) 166–172.
[43] C. Wang, J. Du, H. Wang, C. ’e Zou, F. Jiang, P. Yang, Y. Du, A facile electrochemical sensor based on reduced graphene oxide and Au nanoplates modified glassy carbon electrode for simultaneous detection of ascorbic acid, dopamine and uric acid, Sens. Actuators B Chem. 204 (2014) 302–309.
[44] J. Jiang, X. Du, Sensitive electrochemical sensors for simultaneous determination of ascorbic acid, dopamine, and uric acid based on Au@Pd-reduced graphene oxide nanocomposites, Nanoscale. 6 (2014) 11303–11309.
[45] J.C. Fanguy, C.S. Henry, The analysis of uric acid in urine using microchip capillary electrophoresis with electrochemical detection, ELECTROPHORESIS. 23 (2002) 767–773.
[46] F.T. Thorpe, Ascorbic acid in urine, Br. Med. J. 1 (1938) 542.
[47] Damm, H.C., Handbook of clinical laboratory data, The Chemical Rubber Company, Cleveland, 1965.
[48] Kissinger, P.T., Pachla, L.A., Reynolds, LD., Wright, S., Analytical methods for measuring uric acid in biological samples and food products, 1987 J Assoc Anal Chem 70 P1.

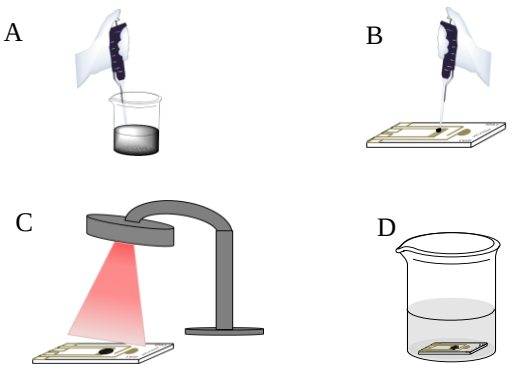

Figure 1. Schematic illustration of the preparation procedure of the sensor described in this study: A) AuNPs-GO dispersion. B) Addition of 0.5 μL of AuNPs-GO dispersion on Au-IDA electrode. C) Drying by IR lamp and D) Storage in PBS (0.25 M, pH 7.0) until its use.

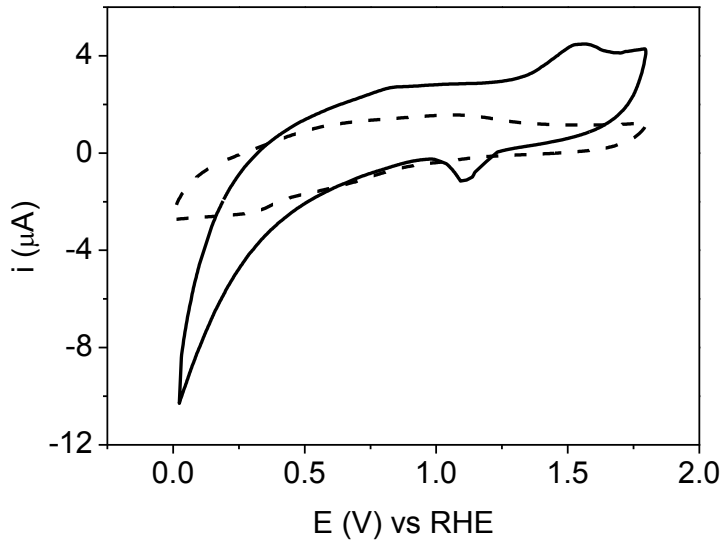

Figure 2. Steady state voltammograms in PBS (0.25 M, pH 7.0), $v_{scan} = 0.1$ V s^{-1}. Electrodes used: GO/Au-IDA (dashed line) and AuNPs-GO/Au-IDA (solid line).

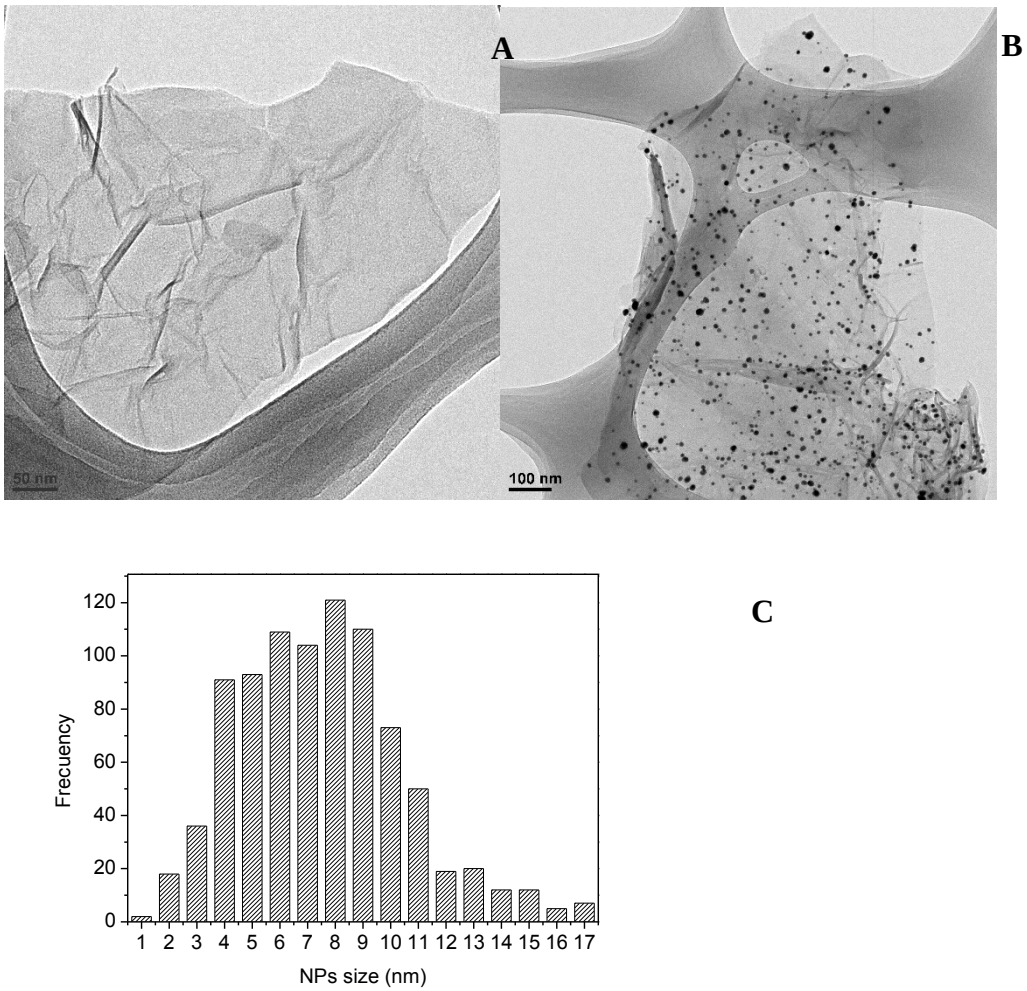

Figure 3. TEM images of: A) GO dispersion; B) AuNPs-GO dispersion and C) histogram of gold nanoparticles size.

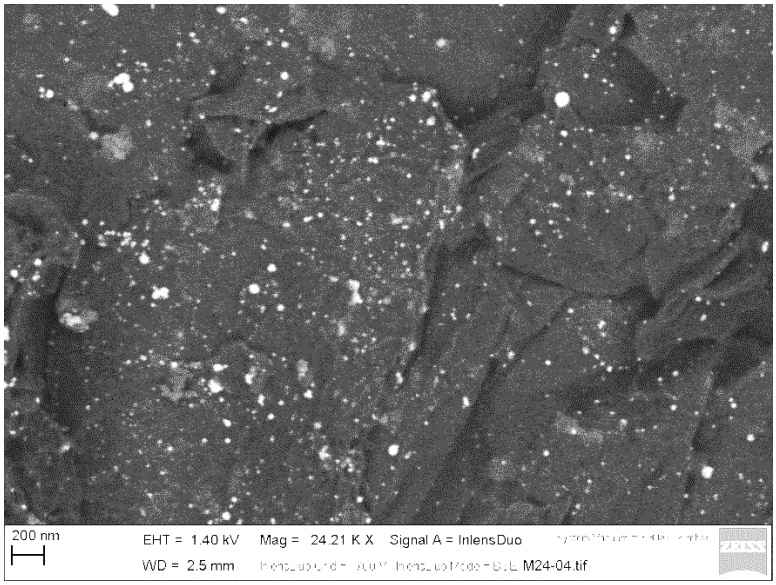

Figure 4. FE-SEM image for AuNPs-GO/Au-IDA modified electrode.

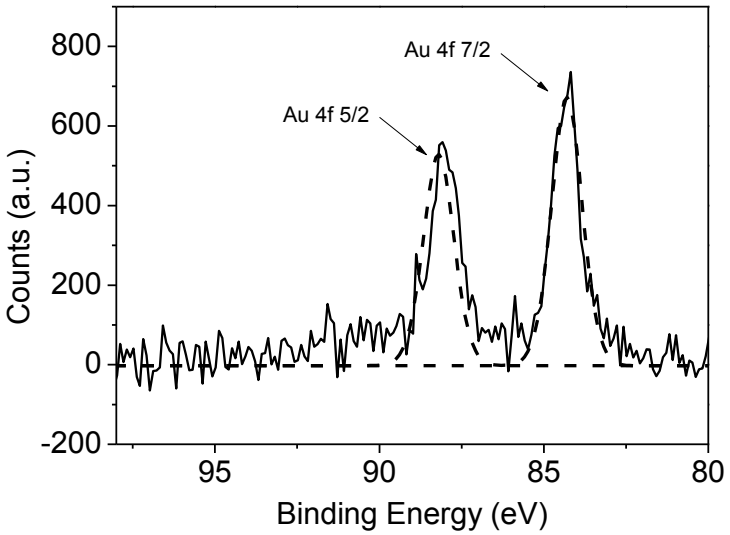

Figure 5. Au $4f_{7/2}$ and Au $4f_{5/2}$ XPS spectra for AuNPs-GO dispersion.

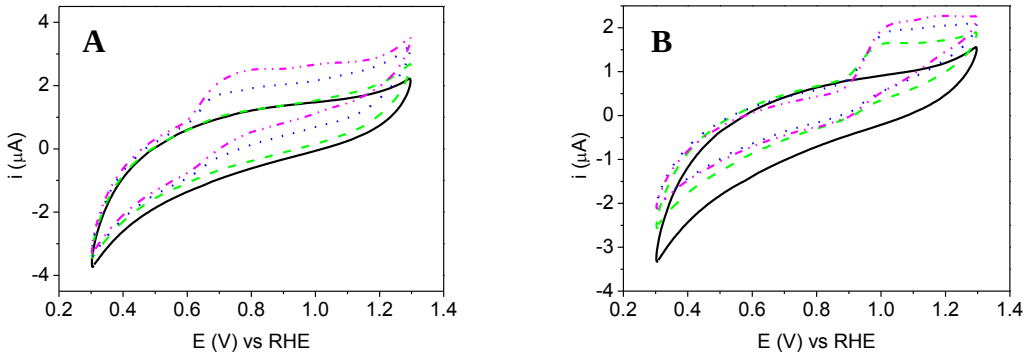

Figure 6. Cyclic voltammograms for AuNPs-GO/Au-IDA electrode for: A) different AA concentrations: 0 μM (black solid line), 75 μM (green dashed), 175 μM (blue dotted), and 275 μM (pink dashed dotted); B) different UA concentrations: 0 μM (black solid line), 200 μM (green dashed), 400 μM (blue dotted), and 600 μM (pink dashed dotted), v_{scan} = 0.1 V·s^{-1}. Electrolyte: PBS (0.25 M, pH 7.0)

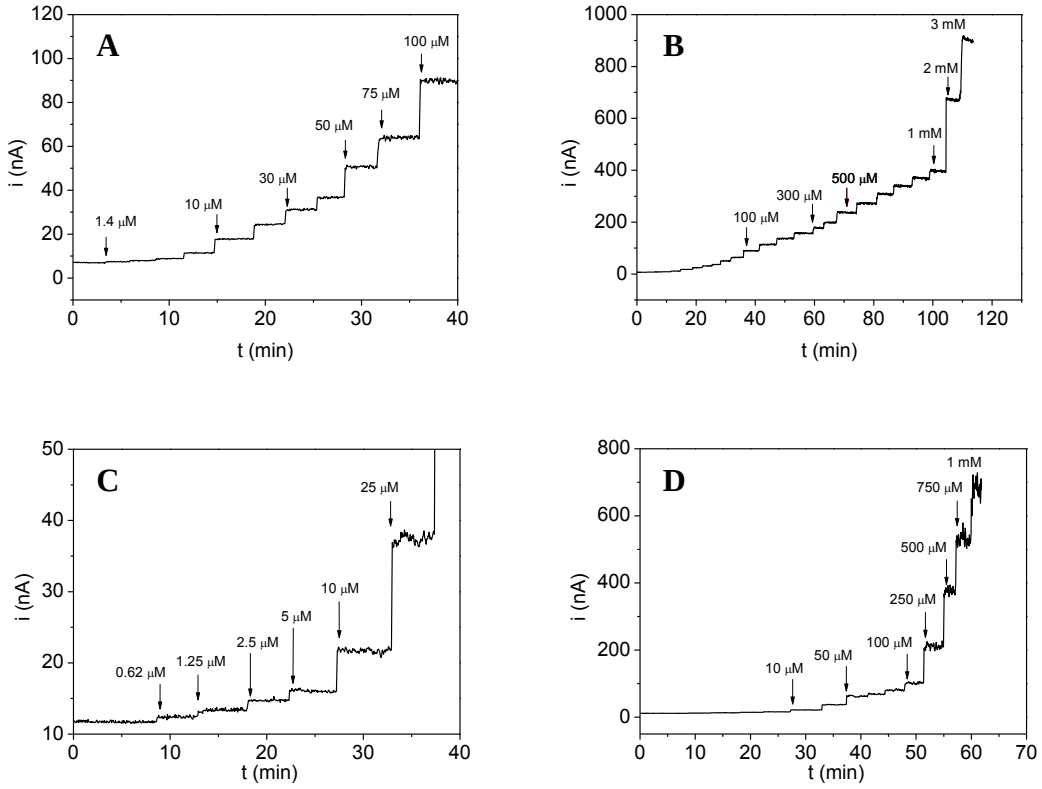

Figure 7. Amperometric responses for AuNPs-GO/Au-IDA electrode to successive additions of: A-B) AA at 0.75 V, C-D) UA at 1.0 V in stirred PBS (0.25 M, pH 7.0). E_i = 0.5 V.

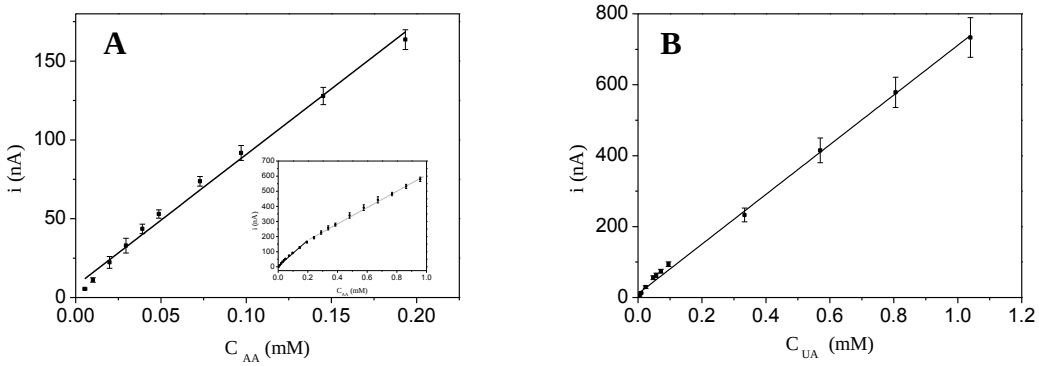

Figure 8. Calibration curves for AuNPs-GO/Au-IDA modified electrodes towards: A) AA additions. Inset: ; B) UA additions. Data corresponding to Figure 7.

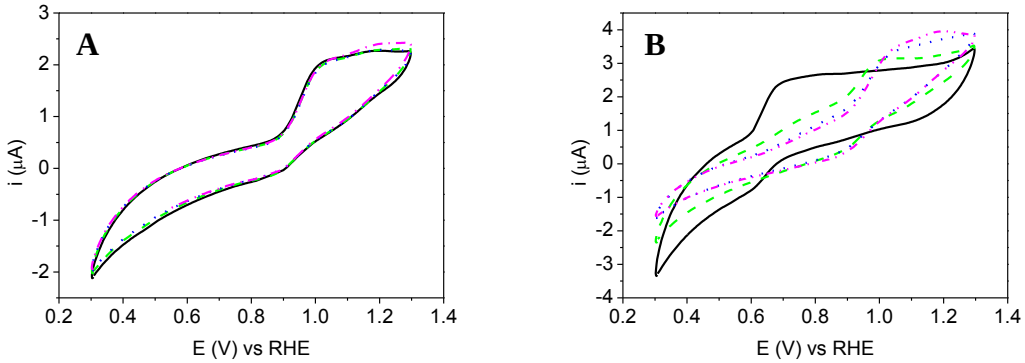

Figure 9. Cyclic voltammograms of AuNPs-GO/Au-IDA modified electrode for successive additions of: A) AA on a solution of UA 600 μM (black solid line: 0 μM AA ; green dashed: 30 μM AA; blue dotted: 60μM AA; pink dashed dotted: 90 μM AA; B) UA on a solution of AA 275 μM (black solid line: 0 μM UA; green dashed: 200 μM UA; blue dotted: 400 μM UA; pink dashed dotted: 600 μM UA). Electrolyte : PBS (0.25 M, pH 7.0)

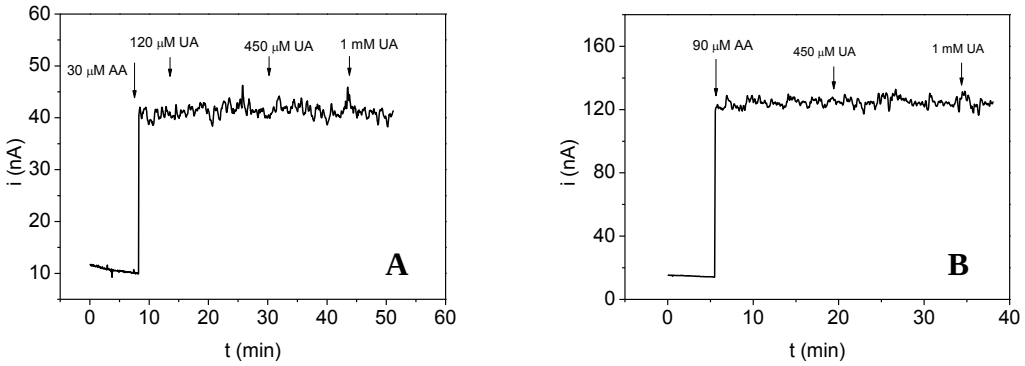

Figure 10. i-t curves obtained for interference study of UA on: A) AA 30 μM; B) AA 90 μM . E_i = 0.5 V, E_f = 0.75 V. Electrode used: AuNPs-GO/Au-IDA. Electrolyte: PBS (0.25 M, pH 7.0)

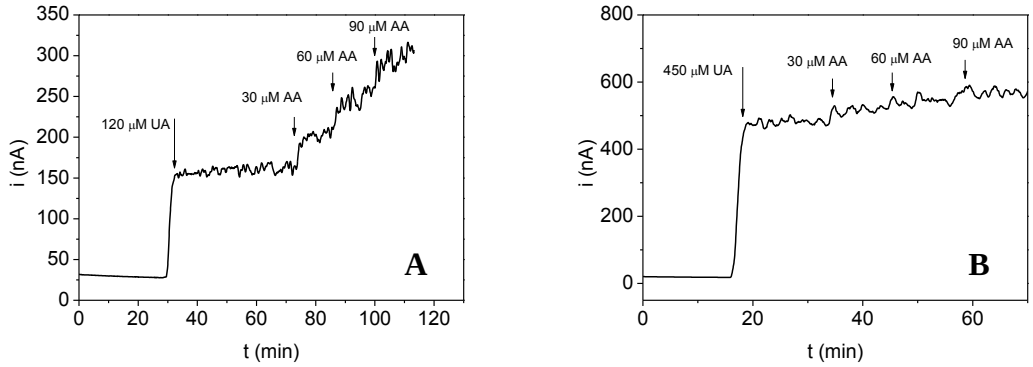

Figure 11. i-t curves obtained for interference study of AA on: A) UA 120 μM; B) UA 450 μM . E_i = 0.5 V, E_f = 1.0 V. Electrode used: AuNPs-GO/Au-IDA. Electrolyte: PBS (0.25 M, pH 7.0)

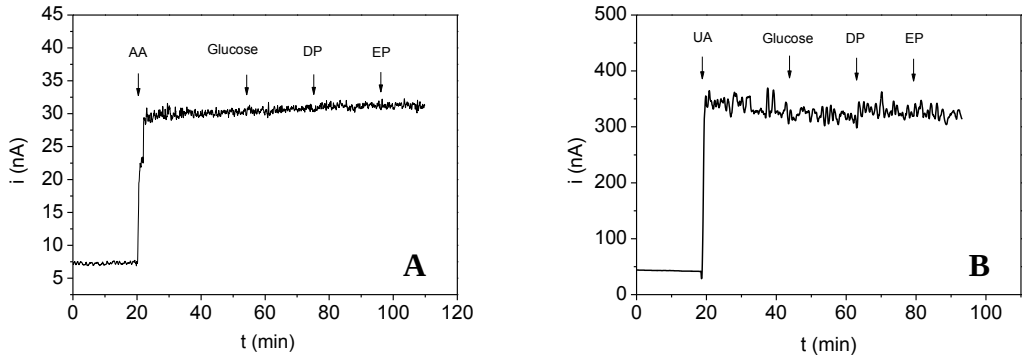

Figure 12. i-t curves for interference study of glucose 5 mM, dopamine 1 μM and epinephrine 0.5 μM on: A) AA solution (50 μM) at 0.75 V; b) UA solution (420 μM) at 1.0 V. E_i = 0.5 V. Electrode used: AuNPs-GO/Au-IDA. Electrolyte: PBS (0.25 M, pH 7.0).

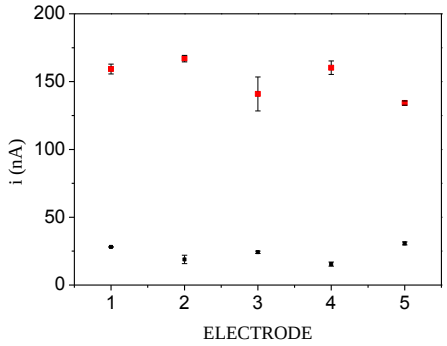

Figure 13. Inter-sensor reproducibility studied on urine sample by chronoamperometry for five electrodes at 0.95 V (black dots) and 1.2 V (red dots). E_i = 0.5 V. Electrode used: AuNPs-GO/Au-IDA. Electrolyte: PBS (0.25 M, pH 7.0).

Table 1. Analytical figures of merit for the quantification of AA and UA by the AuNPs-GO/Au-IDA modified electrode.

Parameter	Analyte	
	AA	UA
Sensitivity ($nA \cdot mM^{-1}$)	830 ± 60	728 ± 16
Intercept (nA)	7 ± 5	13 ± 7
r	0.996	0.999
N	10	12
n	3	3
Working range (μM)	4.6-193	2-1000
LOD (μM)	1.4	0.62
LOQ (μM)	4.6	2
CV (%) (n = 3; 20 μM)	16	13

Table 2. Comparison of analytical characteristics for several electrochemical AA, and UA sensors.

	Detection Limit (μM)		Linear Range (μM)		Ref.
	AA	UA	AA	UA	
Mesoporous nitrogen rich carbon/GCE	0.01	0.01	1 - 700	0.01 - 80	[38]
Cysteine sonogel-carbon modified electrode	50	10	50-100	10-100	[39]
$[Ni(phen)_2]^{2+}$-SWCNTs/GCE	12	0.76	30-1546	1-1407	[40]
CNF-CPE	2	0.2	2-64	0.8-16.8	[41]
Reduced graphene oxide/GCE	300	0.5	500-2000	0.5-60	[42]
AuRGO/GCE	51	1.8	240-1500	8.8-53	[43]
Au@Pd-RGO/GCE	0.02	0.005	0.1-1000	0.02-500	[44]
AuNPs-GO/GCE	200	20	200-800	20-260	[22]
AuNPs-GO/Au-IDA	1.4	0.62	4.6-193	2-1000	This work